Paper presented at the 22nd Asian Conference on Remote Sensing, 5 - 9 November 2001, Singapore.

The study on the comparison of ADEOS-II GLI NDVI and other sensors NDVI by using field experiment data

Hirokazu Yamamoto, Hiroki Yoshioka, Karim Batchily, Laerte Ferreira, Alfredo R. Huete, Koji Kajiwara, and Yoshiaki Honda

National Space Development Agency of Japan, Earth Observation Research Center (NASDA/EORC)

1-8-10, Haruhi, Chuo-ku, Tokyo, JAPAN

TEL: +81-3-6221-9068

FAX: +81-3-6221-9192

E-mail: kath@eorc.nasda.go.jp

KEY WORDS: ADEOS-II GLI, NDVI, Global Vegetation Monitoring

ABSTRACT: Environmental monitoring over land surfaces has various complexities caused by highly heterogeneous surface structures with vegetation layer, soil surfaces, and atmospheric disturbance. The vegetation biophysical parameters must be provided with sufficient accuracy to be used as an input of general circulation models, where the satellite remote sensing also plays an important role. Satellite remote sensing is the use of vegetation index (VI) as an intermediate variable to quantify status and amount of vegetation from satellite images. Various VI products currently exist and more VI products are expected to be available simultaneously, the estimation of biophysical parameters through VI has to be compatible by various sensors to ensure continuity of global environmental simulation over generations. Therefore, it is important to investigate the compatibility of VI products for new sensors with existing and old satellite sensors every time a new satellite will be launched. A soon to be launched optical sensor on board Japanese ADEOS-II platform, named Global Imager (GLI), is the focus of this study.

1. Introduction

The vegetation biophysical parameters must be provided with sufficient accuracy to be used as an input of general circulation models, where the satellite remote sensing also plays an important role. Satellite remote sensing is the use of vegetation index (VI) as an intermediate variable to quantify status and amount of vegetation from satellite images. Various VI products currently exist and more VI products are expected to be available simultaneously, the estimation of biophysical parameters through VI has to be compatible by various sensors to ensure continuity of global environmental simulation over generations. Therefore, it is important to investigate the compatibility of VI products for new sensors with existing and old satellite sensors every time a new satellite will be launched. A soon to be launched optical sensor on board Japanese ADEOS-II platform, named Global Imager (GLI), is the focus of this study.

2. Objective

The objective of this study is to investigate the compatibility of GLI vegetation index products (250m and 1km spatial resolution), normalized difference vegetation index (NDVI) with LANDSAT 7- ETM+, TERRA-MODIS,

NOAA14-AVHRR over several EOS core sites, including Mongolian grassland (Semi arid), Konza (Tall grassland prairie), and Brasilia National Park.

3. ADEOS-II GLI

The Global Imager (GLI) is on boarded the ADEOS-II satellite, which will be launched on Feb., 2002. The objective of this satellite is to acquire data contributing for international global climate change research, as well as for application such as meteorology and fishery. ADEOS-II is particularly dedicated to water and energy cycling and carbon cycling. GLI sensor is an optical sensor for observing globally and so frequently the reflected radiance of land, ocean, and cloud. Data obtained by this satellite sensor may be used for understanding the global circulation of carbon, monitoring cloud, snow, ice, and sea surface temperature, and grasping the primary marine production. GLI is an advanced type of the mission of Ocean Color and Temperature Scanner (OCTS) on-board ADEOS for further expansion of observation. And this sensor has spatial resolution of 1km and 250m, and has 23 channels in visible and near-infrared region (VNIR), 5 channel in short-wave length infrared region (SWIR), and 7 bands in middle and thermal infrared region for its multispectral observation. Although the ground resolution is at the nadir of 1km, a part of the bands in VNIR and SWIR has a resolution of 250 m at the nadir that will be used for observing vegetation and cloud. The observation region by mechanically scanning is 12 picture elements (12 km) to the forward direction and 1600 km in the cross-track direction. (See Table 1)

4. Field Experiment Site and Calculation Methods

4.1 Mandalgovi

The study area is around Mandalgobi in Mongolia (See Figure.1), which is the EOS core site. Measurement in three types of grassland was conducted around Mandalgobi. First observation site, Site 1 is located in north side of Mandalgobi (N45deg59min41.5sec E106deg19min39.5sec) and this site is more dense vegetated area than other site . Measurement in this site is conducted during 3-9 Aug., 1998, Second site, Site 2 is located in western side of Mandalgobi (N45deg38min51.9sec E105deg39min13.3sec) and this is sparse vegetated grassland area, and data is obtained in Aug. 10,1998. Third site, Site 3 is located in southern side of Mandalgobi (N45deg23min23.6sec E106deg14min9.9sec) and measurement was conducted 11 Aug., 1998. Data obtained by mobile measurement system is used in this study. Spectrometer (Soma Optics Inc) can measure in visible/near infrared between 350nm and 1050nm (measured with 512ch. mode). This measurement is conducted by Chiba University's group.

4.2 The Brasilia National Park

The BNP, which is the largest LBA core site in the Cerrado biome, is located in the northern Federal District, Brazil, between 15deg35min and 15deg45min south latitude and 47deg53min and 48deg05min west longitude (Figure 2). Major land cover types in the BNP site is cerrado grassland, the herbaceous dominated region, shrub cerrado, mostly a mixture of grasses and shrubs, wooded Cerrado, with the predominance of shrubs over trees in the woody layer, cerrado woodland, densely covered by trees, and last is gallery forest, a riparian type of vegetation. The field campaign is conducted by Arizona University's group from April to 5 May, and this study reports the results of May 5 data. Spectroradiometric data was obtained by light type airborne measurement. The spectrometer is ASD FieldSpec HH, which is able to measure from 270nm to 1070nm.

4.3 Konza

Konza is located in the Flint Hills region of northeastern, which is the EOS core site (Figure 3). The vegetation of Konza Prairie is predominately native tallgrass prairie, dominated by the perennial, warm-season grasses big bluestem, little bluestem, Indiangrass, and switchgrass. The field campaign is conducted by Arizona University's group from June 13 to 16, and this study reports the results of June 15 data. SpectroRadiometer data was obtained by Ground measurement. The spectrometer is ASD FieldSpec HH, which is able to measure from 270nm to 1070nm.

4.4 Radiometric data processing

Band-Averaged reflectance is calculated in this study. The focused satellite sensors are NOAA14/AVHRR, Landsat7/ETM+, GLI narrow bands(ch.13 and 19), GLI board bands (ch.22 and ch.23),Terra/MODIS, and Seastar/SeaWiFS. Full resolution spectral reflectance is convolved with each satellite sensors. The band-averaged reflectance is calculated as the following equation,

$$R_{sat} = \frac{\int_{\lambda_1}^{\lambda_2} B(\lambda) R(\lambda)\, d\lambda}{\int_{\lambda_1}^{\lambda_2} B(\lambda)\, d\lambda} \quad (1)$$

where R_{sat} is band-averaged reflectance, $B(\lambda)$ is Relative Spectral Response, and $R(\lambda)$ is spectral reflectance. Therefore NDVI is able to be calculated by

$$NDVI = \frac{NIR - Red}{NIR + Red} \quad (2)$$

where NIR is the spectral reflectance in the near-infrared range, Red is the spectral reflectance in the visible red range.

5. Results

Figure.5 shows scatter plot of AVHRR NDVI vs. ETM+, GLI1 (narrow band), GLI2 (broad band), MODIS, and SeaWifs NDVI using spectral reflectance at Mandalgobi and Konza. ETM+, GLI1 (narrow band), GLI2 (broad band), MODIS, and SeaWifs NDVI are different from AVHRR NDVI. Figure.6 shows scatter plot of AVHRR NDVI vs. ETM+, GLI1 (narrow band), GLI2 (broad band), and MODIS NDVI using spectral reflectance at Mandalgobi. In over 0.20 of AVHRR NDVI, ETM+, GLI1 (narrow band), GLI2 (broad band), and MODIS NDVI are higher than AVHRR NDVI. On the other hand, at approx. 0.11 of AVHRR NDVI, ETM+, GLI1 (narrow band), GLI2 (broad band), and MODIS NDVI are lower than AVHRR NDVI. Figure.7 shows scatter plot of AVHRR NDVI vs. ETM+, GLI1 (narrow band), GLI2 (broad band), and MODIS NDVI using spectral reflectance at Konza. ETM+, GLI1 (narrow band), GLI2 (broad band), and MODIS NDVI are higher than AVHRR NDVI. It is investigated the compatibility of GLI NDVI with ETM+, MODIS, AVHRR NDVI. Table.2 shows NDVI value of Average and standard deviation for each vegetation type. It is clear that GLI1 is different from other sensors.

6. Conclusions

1. GLI narrow band NDVI is different from other NDVI. In case of dense vegetated area, NDVI value is highest, and the difference from AVHRR NDVI value is approx. 0.11. On the other hand, in case of sparse vegetated area (AVHRR NDVI is less than 0.20), it is lower value than other VIs.

2. GLI broad band NDVI is quite similar to ETM+ and MODIS sensor's NDVI. This indicates that it is able to compare with global biophysical maps obtained from the different scale satellite data.

ACKNOWLEGMENT

The authors would like to thank all the contributions form both Dr. Huete's group (Karim Batchliy, Fricky Keita et al., Laerte Ferreira) and Dr. Honda's group(Asako Konda et al.) for the data collection during the field campaigns. This work was supported by NASDA GLI grants (Dr. A.R. Hute and Dr. Y.Honda).

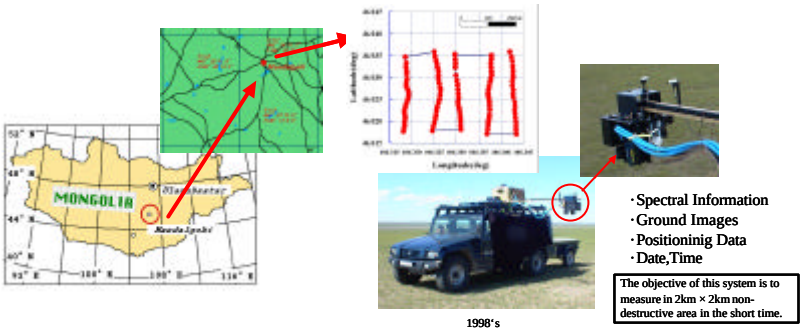

Figure 1. Mandalgovi Measurements (by Chiba Univ.)

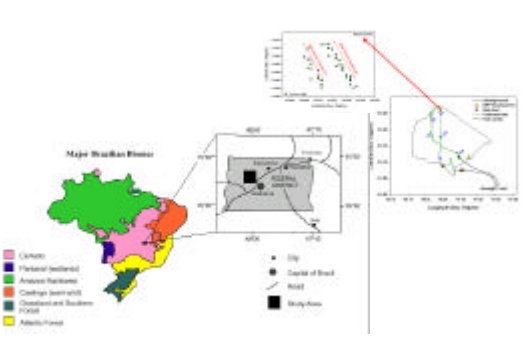

Figure 2. BNP Measurement (by Arizona Univ.)

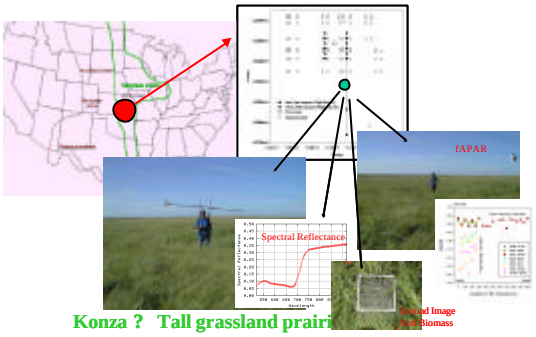

Figure 3. Konza Measurement (Arizona Univ.)

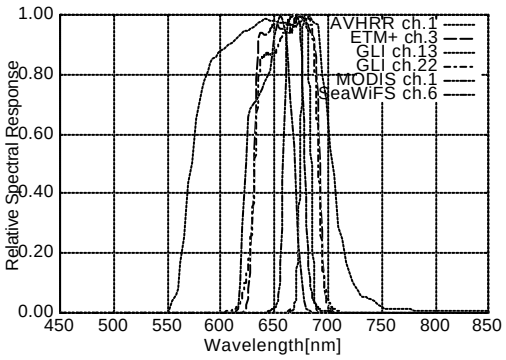

(a)Red Bands

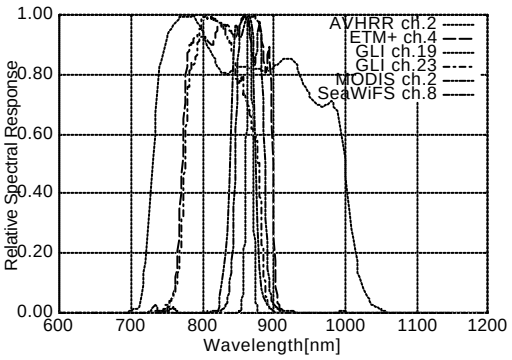

(b)NIR Bands

Figure.4 Band Pass Filters

Table.1 GLI Bands for Land studies

1km Resolution			250 m Resolution		
Band #	Center(Width)	Use	Band #	Center (Width)	Use
Ch1	380(10)	OAC	Ch20	460(70)	LAC
Ch2	400(10)	O	Ch21	545(50)	LAC
Ch3	412(10)	O	Ch22	660(60)	LAC
Ch4p	443(10)	OLAC	Ch23	825(110)	LAC
Ch5p	460(10)	OLAC	Ch28	1640(200)	LAC
Ch6	490(10)	O	Ch29	2210(220)	LAC
Ch7p	520(10)	OAC			
Ch8p	545(10)	OAC			
Ch9	565(10)	OL			
Ch10	625(10)	O			
Ch11	666(10)	O			
Ch12	680(10)	O			
Ch13	678(10)	LAC			
Ch14	710(10)	O			
Ch15	710(10)	LAC			
Ch16	749(10)	O			
Ch17	763(8)	LA			
Ch18	865(20)	O			
Ch19	865(1)	LAC			
Ch24	1050(20)	LAC			
Ch25	1135(70)	A			
Ch26	1240(20)	LAC			
Ch27	1380(40)	A			

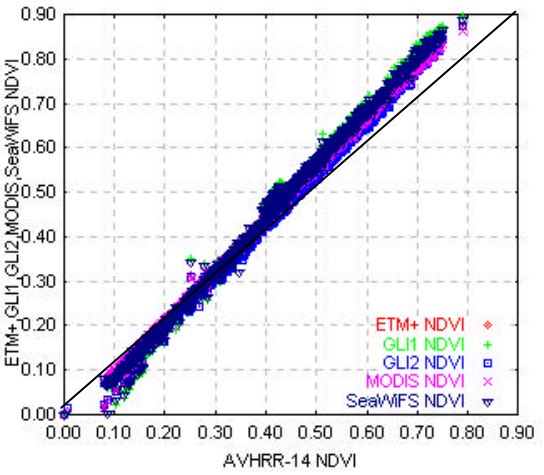

Figure.5 Scatter plot of

AVHRR NDVI vs. ETM+,GLI1,GLI2

MODIS and SeaWifs NDVI (Mandalgovi + Konza)

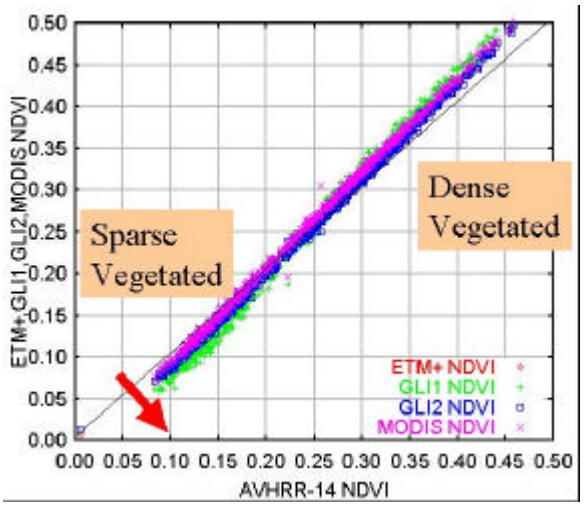

Fig.6 Scatter plot of
AVHRR NDVI vs. ETM+,GLI1,GLI2
MODIS NDVI (Mandalgovi)

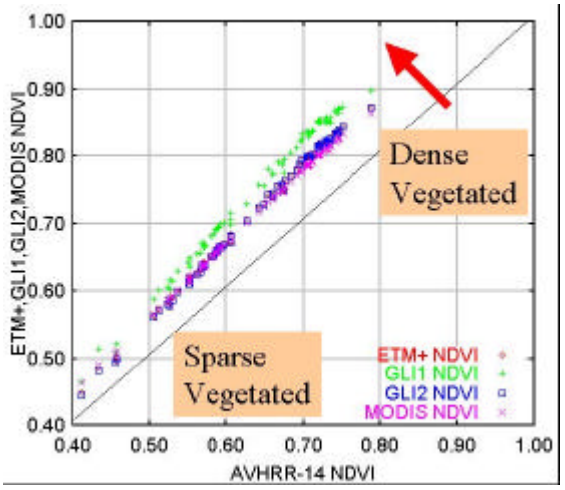

Figure.7 Scatter plot of
AVHRR NDVI vs. ETM+,GLI1,GLI2
MODIS NDVI (Konza)

Table.2 NDVI value of Average and standard deviation for each vegetation type

Mongolia(slightly dense)					
	AVHRR14	ETM	GLI1 (narrow)	GLI2 (broad)	MODIS
AVE.	0.316	0.334	0.338	0.333	0.340
Std.	0.073	0.082	0.100	0.079	0.083
Mongolia(Sparse)					
	AVHRR14	ETM	GLI1 (narrow)	GLI2 (broad)	MODIS
AVE.	0.161	0.156	0.145	0.156	0.162
Std.	0.050	0.056	0.062	0.056	0.056
Konza(dense)					
	AVHRR14	ETM	GLI1 (narrow)	GLI2 (broad)	MODIS
AVE.	0.634	0.713	0.743	0.711	0.707
Std.	0.087	0.101	0.105	0.102	0.095